Proton-Coupled Electron Transfer Involving Tyrosine Z in Photosystem II†

Henriette Kühne‡,|| and Gary W. Brudvig*,§

Departments of Chemistry and Molecular Biophysics & Biochemistry, Yale University, P.O. Box 208107, New Haven, Connecticut 06520-8107

Received: March 5, 2002; In Final Form: June 4, 2002

The O_2-evolving complex (OEC) of photosystem II (PSII) catalyzes the oxidation of water to dioxygen. In addition to a tetramanganese-oxo (Mn_4) cluster, calcium and chloride ions, the OEC also contains Tyrosine Z (Y_Z), a redox intermediate in the water oxidation reaction. The redox mechanism employed by Y_Z is under much debate. Using a novel method to study Y_Z oxidation based on the kinetic competition with secondary donors, we examine the electron-donation pathways of manganese-depleted PSII over a range of temperature and pH. H/D substitution causes a shift in the onset temperature for Y_Z oxidation, enabling measurements of lyonium isotope effects. In deuterated samples, the onset temperature for Y_Z oxidation is upshifted, suggesting that proton movement is a required step. Proton inventory experiments were performed to determine the number of protons that shift during the Y_Z oxidation reaction. Our findings indicate the movement of a single proton during the rate-limiting step of the oxidation process. The results presented herein demonstrate a need for proton movement in conjunction with Y_Z oxidation and support previous proposals that a proton-coupled electron transfer (PCET) step is necessary for oxidation of Y_Z. The possible involvement of PCET in the energetics of specific steps in the mechanism of water oxidation is discussed.

Introduction

Photosystem II (PSII) is a transmembrane protein complex that contains a number of redox-active species and carries out the initial steps in oxygenic photosynthesis. Its O_2-evolving complex (OEC) contains a tetramanganese-oxo (Mn_4) cluster and catalyzes the oxidation of water to molecular oxygen. Following photon absorption by the photoactive chlorophyll (P680), a charge separation occurs. Electrons are transferred from the Mn_4 cluster at the donor side of PSII, via a nearby redox-active tyrosine residue (Y_Z), to a diffusible quinone at the acceptor side. Oxidizing equivalents accumulate at the Mn_4 cluster in a cycle of four consecutive oxidation states called S_i states, as the OEC progresses from the S_0 to the S_4 state. Molecular oxygen is released in the S_4-to-S_0 transition. The mechanism by which electrons are abstracted from water is not well understood. Although the Mn_4 cluster plays a central role in O_2 evolution, several other species also are vital to the function of OEC. Both calcium and chloride ions are required for maximal O_2-evolution activity.[1] Furthermore, Y_Z (Y161 of the D1 polypeptide)[2−4] and H190 of the D1 polypeptide[5−9] are located in close proximity to the Mn_4 cluster and are thought to participate directly or indirectly in the electron-transfer mechanism between the Mn_4 cluster and $P680^+$.

Several mechanisms for electron transfer during Y_Z oxidation and $Y_Z^\bullet$ reduction may be envisioned. Oxidized Y_Z exists as a neutral phenoxyl radical, $Y_Z^\bullet$.[10−12] Its reduced form may exist as a tyrosinate anion (Y_Z^-) or neutral tyrosine (Y_Z). If the former case, Y_Z^- oxidation and subsequent $Y_Z^\bullet$ reduction would be proton-independent, with Y_Z bearing a formal negative charge in its reduced state and an unpaired electron in its oxidized state. On the basis of chlorophyll-absorption band shifts during Y_Z oxidation and $Y_Z^\bullet$ reduction, Junge and co-workers argue that Y_Z promotes water oxidation by an electrostatic interaction and acquires a formal charge during reduction.[13,14] However, the band shifts observed may originate from mechanisms other than the transient positioning of a formal charge on Y_Z, such as structural changes in the OEC to accommodate electronic movements.[15] Structural changes within the OEC may include variations in protonation state, shifts in hydrogen bonding, or adjustments in the orientation of dipoles. Similarly, changes in the coordination of the Mn_4 cluster may affect the surrounding protein, causing absorption-band shifts. Therefore, the evidence for a tyrosinate mechanism based on band shifts is not conclusive. Alternatively to existing as a tyrosinate anion, reduced Y_Z may carry a neutral charge. Indeed, FTIR measurements indicate that reduced Y_Z is protonated and, therefore, uncharged.[12] In this case, a proton would have to move during Y_Z oxidation and $Y_Z^\bullet$ reduction. This raises the possibility of proton-coupled electron transfer (PCET, see Scheme 1) during

SCHEME 1: Model for Proton-Coupled Electron Transfer (PCET) from and to Y_Z. A Proton Is Shuttled to and from a Proximal Acceptor Base, to Which it May be Connected by a Hydrogen Bond

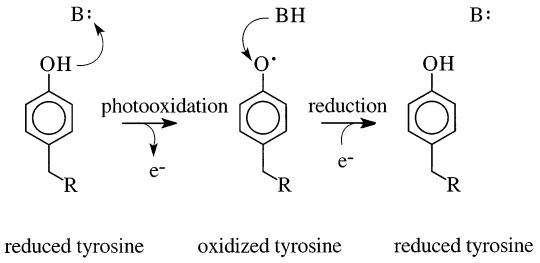

† Part of the special issue "John C. Tully Festschrift".

* To whom correspondence should be addressed. E-mail: gary.brudvig@yale.edu; Phone: (203) 432-5202; Fax: (203) 432-6144.

‡ Department of Molecular Biophysics & Biochemistry.

§ Department of Chemistry.

|| Current address: Magellan Pharmaceutical Development, 9250 Trade Place, San Diego, California 92126

10.1021/jp0206222 CCC: $22.00
Published on Web 07/09/2002

the photooxidation of Y_Z and the subsequent abstraction by $Y_Z^\bullet$ of a hydrogen atom from water bound to the Mn_4 cluster.[16−21]

It has been shown previously in manganese-depleted PSII that negatively charged electron donors are poor reducing agents of $Y_Z^\bullet$, whereas neutral donors are more efficient at reducing $Y_Z^\bullet$.[22,23] In the past, these results have been interpreted in terms of a repulsion between the externally added reductant and negatively charged groups surrounding Y_Z on the lumenal side of PSII.[23] However, more recent evidence supports the hypothesis that an electron donor's efficiency is determined by its ability to undergo PCET rather than its charge. For example, $Y_Z^\bullet$ reduction in the presence of diprotonated acids is faster than in the presence monoprotonated acids, even if both carry the same formal charge.[23]

There are two possible models for proton and electron transfer from and to Y_Z (for review, see[21]). Which mechanism prevails may vary as the OEC advances through the S-state cycle.[7,8,21,24] In one model, concerted electron and proton transfer occur, as both electrons and protons are transferred from the Mn_4 cluster to $Y_Z^\bullet$ during its reduction. This mechanism requires significant proton movement and is expected to exhibit noticeable isotope and temperature effects. In the second model, electron and proton transfer occur consecutively as electrons are passed to $P680^+$ and acquired from the Mn_4 cluster, and protons are shuttled between Y_Z and the hydrogen-bonded D1-H190 imidazole moiety. It has been proposed that transfer of a proton to D1-H190 is followed by deprotonation of the distal nitrogen on the imidazole ring, leading to proton release into the lumenal aqueous space via a chain of proton donors/acceptors. The importance of D1-H190 as the proton acceptor during Y_Z oxidation is supported by measurements of electron transfer in D1-H190-deficient mutants from *Synechocystis*. These studies show that the Y_Z oxidation/$Y_Z^\bullet$ reduction rates are slowed significantly in the absence of the imidazole moiety from D1-H190, but can be partially restored by addition of extrinsic imidazole or other small organic bases.[7] Furthermore, flash-induced chlorophyll fluorescence kinetics studies in manganese-depleted PSII from *C. reinhardtii* indicate that the rate of Y_Z oxidation by $P680^+$ is slowed in D1-H190 mutants, as compared to wild-type PSII.[8] Both studies conclude that Y_Z is a more efficient electron donor to $P680^+$ if D1-H190 (or imidazole or another small base) can act as a temporary acceptor to the Y_Z hydroxyl proton. These findings suggest that Y_Z and D1-H190 participate in the same hydrogen-bonding network and that Y_Z oxidation necessitates either concerted or consecutive proton transfer.

If proton/protein movements are required, Y_Z oxidation should be greatly slowed below the protein-glass transition temperature, the minimum ambient temperature required for nonvibrational thermal motions and nuclear rearrangements. Neutron-scattering studies have shown that the dynamic protein-glass transition can occur anywhere between 180 K[25] and 230 K.[26,27] Indeed, photooxidation of alternative non-PCET electron donors is observed below this temperature range in PSII. For example, Chl_Z oxidation occurs at 77 K,[28−30] and the oxidation of a nearby carotenoid dominates at even lower temperatures,[31−33] indicating a low energetic barrier for electron transfer from these alternative donors. Notably, the S_1-to-S_2-state transition is observed at temperatures as low as 140 K.[28,34] Because this transition presumably involves transient Y_Z oxidation, it has been argued that proton movement during Y_Z oxidation/$Y_Z^\bullet$ reduction in the S_1-to-S_2-state transition occurs back and forth between Y_Z and D1-His190 via a well-ordered hydrogen bond.[21] In contrast, Y_Z oxidation in the absence of a functional Mn_4 cluster[35−39] and the S-state transitions other than the S_1-to-S_2-state transition[34,40,41] are observed only at temperatures above 200 K, consistent with significant proton/protein motion in these reactions.

The glass transition temperature is highly dependent on environmental conditions.[27,42,43] In addition, PCET via a well-ordered hydrogen bond can have a very low activation barrier. Therefore, the presence of a proton-accepting moiety to aid PCET might downshift the temperature where Y_Z oxidation remains permissible. In the present study, we examine the effect of pH and lyonium isotope on the temperature at which Y_Z oxidation becomes competitive with Chl_Z oxidation. Although past studies of Y_Z oxidation have focused on direct kinetic measurements, our approach focuses on the relative yield of Y_Z oxidation compared to the competing electron donors. This study follows from previous studies of electron donation by the Mn_4 cluster and cytochrome b_{559} in which the reactions were characterized by measurement of the yields of the competing electron donors.[28,29]

At low pH and in deuterated samples, higher temperatures are required to observe oxidation of Y_Z relative to oxidation of Chl_Z, suggesting that proton movement is a required step in the oxidation of Y_Z. Proton-inventory experiments indicate movement of a single proton during the rate-limiting step. In addition, we characterize further the proton acceptor to Y_Z. Provided that the two are connected by a hydrogen bond, the hydrogen-bonding interaction, and thus, Y_Z oxidation should be disrupted at low pH, where the proton acceptor becomes protonated. If the species in question is D1-His190, as suggested previously,[7−9] then favorability of $Y_Z^\bullet$ formation should titrate with a pK_a characteristic of histidine. In an effort to determine the pK_a of the moiety (or moieties) involved in Y_Z oxidation, we show that this is indeed the case.

Experimental Section

Chemicals and Reagents. 1,4-butane sultone, piperazine, PPBQ, and potassium ferricyanide were purchased from Aldrich. HEPES was from American Bioanalytical. DMSO, EDTA, calcium chloride, ethylene glycol, hydrochloric acid, magnesium chloride (hexahydrate), and sucrose were purchased from Baker. Hydroxylamine was from Eastman Kodak Company. Anhydrous sodium acetate and calcium hydroxide were purchased from Fisher Chemical. Glacial acetic acid, calcium acetate, sodium chloride, and sodium hydroxide were purchased from Mallinckrodt. Bovine serum albumin, MES, and Triton X-100 were purchased from Sigma. All were used without further purification. Stock solutions of PPBQ (25 mM in DMSO) and potassium ferricyanide (100 mM in deionized water) were prepared and frozen until use. The buffer PIPBS was synthesized from piperazine and 1,4-butane sultone, as described by Jermyn.[44,45]

PSII Sample Preparation. PSII membranes were isolated from market spinach leaves following the procedure of Berthold et al.[46] with the modifications of Beck et al.[47] except that thylakoid membranes were not frozen before isolation of the PSII membranes. The membranes were stored at 77 K in resuspension buffer, containing 15 mM NaCl, 20 mM MES, pH 6.0, 30% (v/v) ethylene glycol, at concentrations of approximately 6 to 8 mg of chl ml^{-1}, until use. Manganese-depleted PSII was prepared by hydroxylamine treatment, as described in Tamura and Cheniae.[48] Chlorophyll concentrations were measured according to the method of Arnon[49] on a Perkin-Elmer Lambda 3b Series UV-vis spectrophotometer. Assays for O_2 evolution were performed in a home-built, water-jacketed aluminum chamber maintained at 25 °C by a circulating water

bath, equipped with a YSI Clark electrode and using light from a 1200 W xenon lamp (Oriel) filtered through a 10-cm water filter, a heat absorbing (Schott KG-5) filter and a long pass (Oriel LP 610) filter. Typical O_2-evolution rates were 350 to 500 μmol O_2 (mg of chl)$^{-1}$ h^{-1} for untreated PSII.

Samples for EPR measurements were prepared by two washes with the appropriate buffer (see figure legends for buffer conditions of each individual sample). Each buffer contained 40 mM buffering agent: HEPES, MES, or an equimolar mixture of MES and PIPBS, depending on the nature of the experiment and the pH range surveyed. pL values were measured with a pH electrode using the following correction factor where appropriate: pD = pH meter reading + 0.4.[50] For each of the two washing steps, the samples were suspended in 20 mL buffer, centrifuged, and the pellet resuspended in minimal buffer. Following the washes, 1 or 2 mM ferricyanide and 500 μM DCMU or PPBQ were added, and the samples were transferred to quartz EPR sample tubes. Typical sample concentrations for EPR measurements were 7 to 10 mg of chl ml^{-1}.

EPR Measurements. PSII donor-side radicals were produced by 5 to 10 s illumination at varying temperatures using white light from a 500 W quartz tungsten halogen lamp (Oriel). Illuminations of EPR samples measured at 20 K were performed inside a nitrogen-flow cryostat assembly, followed by rapid cooling in a liquid-nitrogen bath to trap the light-induced radicals. Radicals for time-dependent EPR measurements of signal evolution rates were induced by direct illumination inside the EPR resonant cavity. For this purpose, the tungsten−halogen lamp was fitted with a 10-cm water filter and connected to the resonant cavity with a custom-built Lucite light pipe.[45]

Low-temperature EPR measurements at 20 K were performed on a Varian E-line EPR spectrometer equipped with a TE_{102} cavity and an Oxford Instruments ESR 900 liquid-helium cryostat, and interfaced to a Macintosh IIci computer. EPR spectra of the $Chl_Z^\bullet$ and $Y_Z^\bullet$ EPR signals at 20 K were collected under the following conditions: microwave frequency, 9.28 GHz; microwave power, 0.02 mW; magnetic-field modulation frequency, 100 kHz; magnetic-field modulation amplitude, 4 G. Time-dependent EPR spectra were collected on a Bruker ER 200D-SRC EPR spectrometer equipped with a TM_{110} cavity and interfaced with a Macintosh IIci computer. For measurements between 150 and 190 K, a Bruker nitrogen-flow cryostat was used. Room-temperature steady-state EPR spectra were collected under the following conditions: microwave frequency, 9.68 GHz; microwave power, 10 mW; magnetic-field modulation frequency, 100 kHz; magnetic-field modulation amplitude, 2 G. Time-dependent EPR spectra were collected under the following conditions: microwave frequency, 9.68 GHz; microwave power, 0.5 mW (low temperature) or 5.1 mW (room temperature); magnetic-field modulation frequency, 100 kHz; magnetic-field modulation amplitude, 4 G; instrumental time constant, 0.2 s; data-acquisition rate, 4.0 Hz (low temperature) or 1.0 Hz (room temperature). The formation and decay of the $Y_D^\bullet$ and $Y_Z^\bullet$ EPR signals were monitored as the transient evolution of the low-field hyperfine peak at 3430 G; the formation and decay of the $Chl_Z^\bullet$ EPR signal was monitored at 3445 G, near the baseline-crossing point of the Y$^\bullet$ EPR signals. In each case, the conditions used were verified to be nonsaturating. The intensities of the narrow $Y_Z^\bullet$, $Y_D^\bullet$, and $Chl_Z^\bullet$ EPR signals were calculated by double integration of the spectra. Y$^\bullet$ EPR signal intensities were also approximated as the absolute heights of the derivative EPR signal at 3430 G in the time-dependent EPR spectra. Illuminated-minus-dark difference spectra containing contributions from both $Y_Z^\bullet$ and $Chl_Z^\bullet$ were scaled to an integrated area of one and deconvoluted by quantitative fits to pure spectra of $Y_Z^\bullet$ and $Chl_Z^\bullet$.

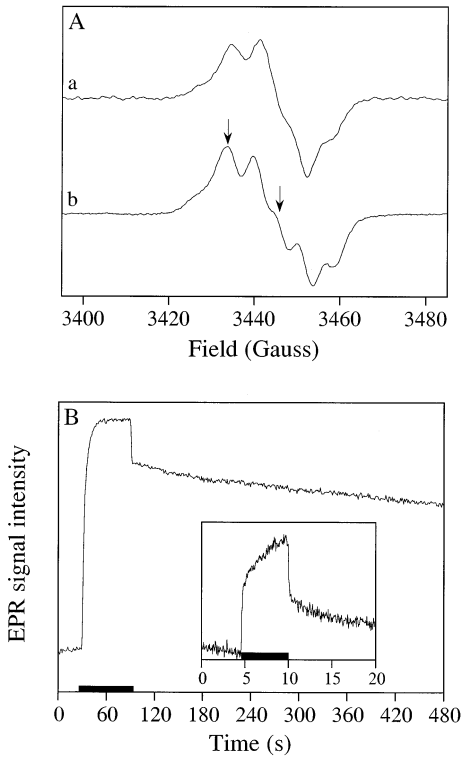

Figure 1. (A) Representative EPR signals from $Y_Z^\bullet$ and $Y_D^\bullet$ in manganese-depleted PSII, recorded at 20 K. (a) dark spectrum, showing $Y_D^\bullet$; (b) illuminated-minus-dark difference spectrum, showing $Y_Z^\bullet$. Illumination was performed at 230 K. The arrow indicates the low-field hyperfine peak position at which time-dependent scans of $Y_Z^\bullet$ intensity were recorded. The sample buffer contained 20 mM MES, 20 mM PIPBS, pH 6.0, 10 mM NaCl, 10 mM $CaCl_2$, 1 mM ferricyanide, and 250 μM DCMU. (B) Light-induced transient radical EPR signal measured at room temperature in manganese-depleted PSII in 40 mM HEPES, pH 7.0, 10 mM $CaCl_2$, 300 mM sucrose, 2 mM potassium ferricyanide and 500 μM PPBQ. The bars denote illumination periods. Main: initial illumination following dark adaptation observed at a magnetic-field position of 3430 G, the resonance position of the low-field hyperfine peak of the Y$^\bullet$ signal; both $Y_D^\bullet$ and $Y_Z^\bullet$ are formed. Inset: subsequent illumination at the same field position; only $Y_Z^\bullet$ is formed.

Results

Figure 1A shows the characteristic EPR signals of $Y_D^\bullet$ and $Y_Z^\bullet$ obtained from manganese-depleted PSII. Both tyrosyl radicals exhibit a ~40-G wide EPR signal centered at g ≈ 2, with similar hyperfine features. $Y_D^\bullet$ is very stable in the dark, whereas $Y_Z^\bullet$ decays quickly with a rate that depends on the state of the OEC.[51] When PSII is subjected to continuous illumination at room temperature, the steady state formed in manganese-depleted or inhibited PSII contains both $Y_D^\bullet$ and $Y_Z^\bullet$, whereas very little $Y_Z^\bullet$ is generated in O_2-evolving PSII under steady-state illumination. We observe $Y_D^\bullet$ to decay single-exponentially in the dark, with a rate constant of 0.1 min^{-1}.[45] A much faster decaying component of the Y$^\bullet$ EPR signal, assigned to $Y_Z^\bullet$, is observed in the initial as well as in subsequent illuminations of manganese-depleted PSII (Figure 1B). These results are in agreement with the finding that repetitive flashes induce rapid formation of a dark-stable $Y_D^\bullet$ EPR signal, whereas the $Y_Z^\bullet$ radical forms only transiently.[52] At lower temperatures where electron donation from Y_Z becomes impaired, steady-

SCHEME 2: Competitive Reduction of $P680^+$ by Donor-Side Redox-Active Species Y_Z and Chl_Z, Following Photoinduced Charge Separation, in Manganese-Depleted PSII Limited to One Turnover in the Presence of DCMU

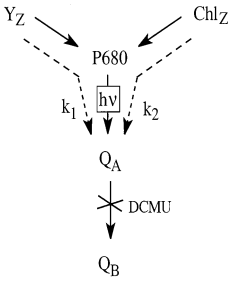

state illumination of manganese-depleted PSII generates a 10-G wide radical EPR signal that is assigned to $Chl_Z^{\bullet}$.[53] Chl_Z is expected to be the main donor in competition with Y_Z over the range of temperatures sampled in this study. It should be noted, however, that the 10-G wide organic radical may include contributions from more than one chlorophyll, as well as from a recently reported carotenoid radical.[31,33,54]

Competitive Formation of $Y_Z^{\bullet}$ and $Chl_Z^{\bullet}$. To address the question of whether electron transfer involving Y_Z is proton-coupled, we studied the competitive formation of $Y_Z^{\bullet}$ and $Chl_Z^{\bullet}$ in manganese-depleted samples limited to a single turnover by DCMU (Scheme 2). Below 200 K, the preferred donor to $P680^+$ is Chl_Z.[28,29] Because electron transfer from Chl_Z to $P680^+$ can still occur at 77 K,[28−30] we presume that the activation barrier for this secondary pathway is very low. Near room temperature, the dominant electron donor to $P680^+$ is Y_Z.[55] Consequently, there will be a temperature range within which both Chl_Z and Y_Z can act as electron donors to $P680^+$ in direct competition with each other, and where electron donation by Y_Z becomes more competitive as the illumination temperature is raised.

Figure 2A depicts a representative plot of illuminated-minus-dark difference EPR spectra containing contributions from both $Y_Z^{\bullet}$ and $Chl_Z^{\bullet}$ EPR signals and recorded at pH 6.5 over a typical range of illumination temperatures. Figure 2B shows the deconvoluted relative yields of $Y_Z^{\bullet}$ and $Chl_Z^{\bullet}$ versus illumination temperature at the same pH. The arrow indicates the temperature at which the contributions from $Y_Z^{\bullet}$ and $Chl_Z^{\bullet}$ are equal, henceforth termed the crossover temperature. Figure 3 shows a plot of the crossover temperature as a function of pH. The crossover temperature decreases sharply at about pH 5.5, i.e., $Y_Z^{\bullet}$ formation remains competitive at lower temperatures as the pH is raised.

This pH dependency may be attributed to three possible sources: effects from the acceptor side, from Chl_Z oxidation, or from Y_Z oxidation. Acceptor-side effects can be ruled out in the presence of DCMU because the single charge separation that can occur involves Q_A as the electron acceptor for all the competing donors. Figure 4 shows that the rate of Chl_Z formation is independent of H/D exchange and that the trapping efficiencies of $Chl_Z^{\bullet}$ and $Y_Z^{\bullet}$ have the same dependencies on temperature and pH. Figure 4A shows the rates of light-induced formation of the $Y_Z^{\bullet}$ and $Chl_Z^{\bullet}$ radicals at pH 5.5 and 7.5 over a range of cryogenic temperatures, where they can easily be resolved on a seconds time scale. At both pH values and over the temperature range sampled, the two rates are found to be linked. Although at low pH, the rates appear temperature independent, at high pH, they increase linearly with temperature, indicating that the rates of $Y_Z^{\bullet}$ (k_1, Scheme 2) and $Chl_Z^{\bullet}$ (k_2, Scheme 2) formation are linked regardless of sample condition. Therefore, we conclude that the competitive yields of $Y_Z^{\bullet}$ and

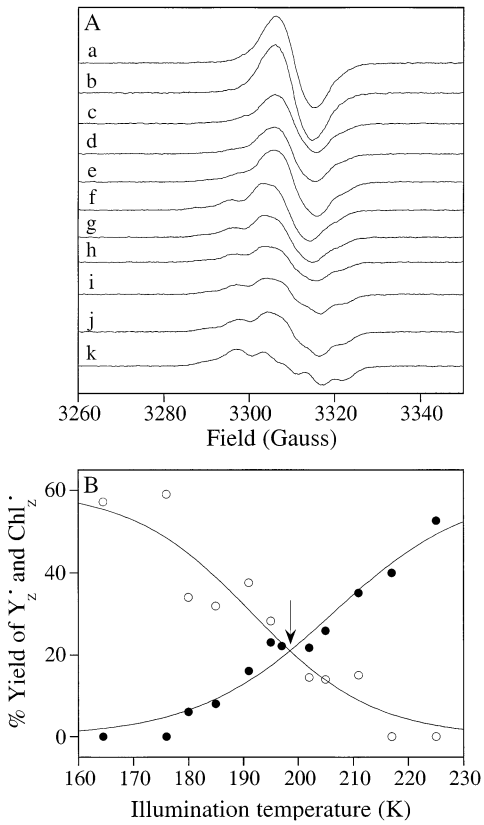

Figure 2. Representative data set for the competitive formation of $Chl_Z^{\bullet}$ and $Y_Z^{\bullet}$ as a function of illumination temperature collected at pH 6.5. Buffer conditions: 20 mM MES, 20 mM PIPBS, 10 mM NaCl, 10 mM $CaCl_2$, 1 mM ferricyanide and 250 μM DCMU. (A) EPR spectra of donor-side radical signals observed at 20 K after illumination over a range of temperatures followed by rapid cooling; (a) 164 K, (b) 176 K, (c) 180 K, (d) 185 K, (e) 191 K, (f) 195 K, (g) 197 K, (h) 202 K, (i) 205 K, (j) 211 K, and (k) 225 K. (B) Yields of (○) $Chl_Z^{\bullet}$ and (●) $Y_Z^{\bullet}$. The solid lines represent sigmoidal fits to the data. The arrow depicts the crossover temperature at which Chl_Z and Y_Z donate to $P680^+$ at equivalent rates.

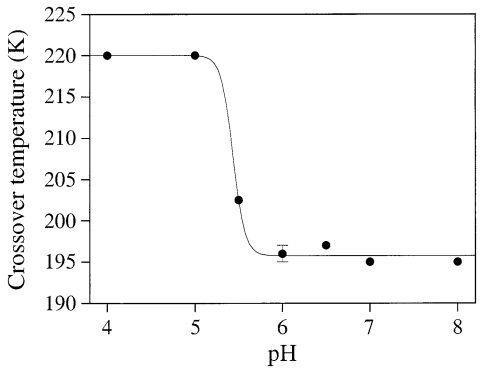

Figure 3. Titration curve of crossover temperature, as defined in Figure 2B, as a function of pH. Buffer conditions: 20 mM MES, 20 mM PIPBS, 10 mM NaCl, 10 mM $CaCl_2$, 1 mM ferricyanide, and 250 μM DCMU.

$Chl_Z^{\bullet}$ represent a direct ratio of the rates at which they are formed. Dark-decay rates were measured consistently at ~0.2 s^{-1} for both radicals at either pH. Because the rate of formation of these species is one or more per second, whereas their rate of decay is approximately one every five seconds, we can assume that the yield is essentially complete during the 5 to 10 s illumination times used in these experiments. Figure 4B shows that the observed effects are not due to a linear increase in the total radical yields formed at high pH. Figure 4C shows that

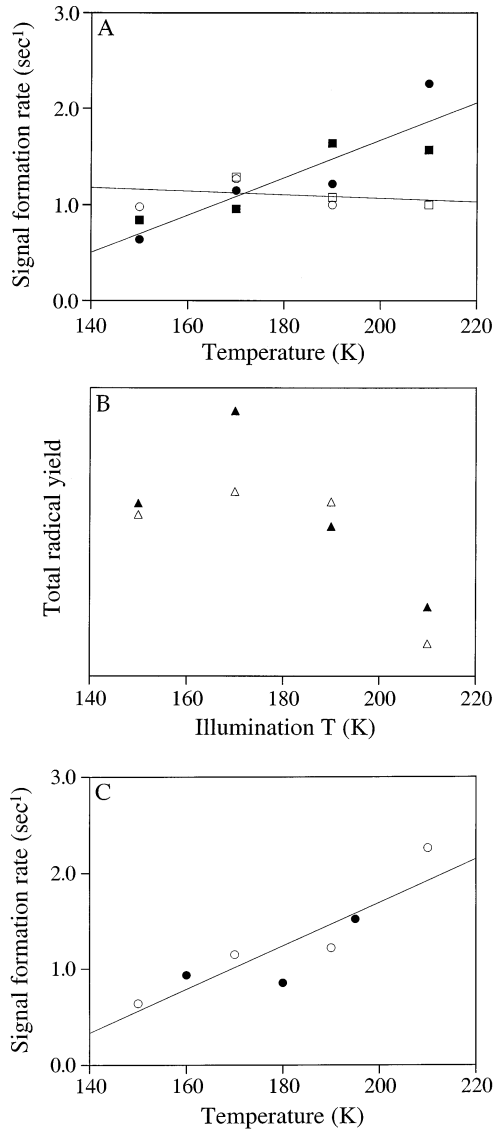

Figure 4. (A) Rates of formation for $Y_Z^{\bullet}$ (squares) and $Chl_Z^{\bullet}$ (circles) at pH 5.5 (open symbols) and 7.5 (filled symbols). The sample buffer contained 20 mM MES, 20 mM PIPBS, 10 mM NaCl, 10 mM $CaCl_2$, 1 mM potassium ferricyanide and 500 mM DCMU. The lines represent linear least-squares fits to all data points at pH 5.5 and 7.5, respectively. (B) Total radical yields ($Y_Z^{\bullet}$ plus $Chl_Z^{\bullet}$) as a function of illumination temperature at pH 5.5 (open triangles) and 7.5 (filled triangles). These yields are estimated from the relative heights of the transient signal formed as a steady state is established during continuous illumination. (C) Isotope effect on the rate of $Chl_Z^{\bullet}$ build-up in the steady state under continuous illumination in the presence of hydronium (pH 7.5, open cicles) and deuterium (pD 7.0, filled cicles). The line represents a linear least-squares fit to all points. Buffer conditions were 40 mM MES, 10 mM NaCl, 10 mM $CaCl_2$, 300 mM sucrose, 1 mM ferricyanide, and 250 mM DCMU.

Chl_Z oxidation is also independent of H/D substitution, as is evidenced by the absence of an H/D isotope effect on the $Chl_Z^{\bullet}$ radical formation rate over the temperature range examined.

From these results, we conclude that the observed pH dependency does not result from acceptor-side effects or from effects on Chl_Z oxidation. This leaves Y_Z oxidation as the source of the observed pH dependence. The pH dependence indicates that photooxidation of Y_Z is proton coupled and that the phenolic hydroxyl proton of Y_Z is donated to a proximal base in the formation of the $Y_Z^{\bullet}$ radical. The observed titration behavior may be attributed to the protonation of a donor-side base below pH 6. A similar pH dependency has been observed in a comparison of manganese-depleted PSII to a Y_Z-less mutant, which showed that at pH 8.5 $P680^+$ reduction by both Y_Z and Y_D occurs at extremely fast rates, whereas at pH 6.5 both rates are significantly slowed.[52] The retardation of Y_D oxidation at low pH is much more pronounced that than of Y_Z,[52] indicating that the environment of Y_Z is specifically configured to enhance its oxidation at moderately low pH.

Activation Barriers to $Y_Z^{\bullet}$ Formation. The fractional yields of $Y_Z^{\bullet}$ and $Chl_Z^{\bullet}$ are representative of their respective rates of formation. Because the initial rates are reflected in the relative yields of $Y_Z^{\bullet}$ and $Chl_Z^{\bullet}$ formed, the ratio of the measured yields is directly proportional to the ratio of the rate constants k_1 and k_2 (eq 1 and Scheme 2)

$$\frac{[Y_Z^{\bullet}]}{[Chl_Z^{\bullet}]} = \frac{k_1}{k_2} \tag{1}$$

In the presence of DCMU, each reaction center will form a single stable charge separation in which the donor is either Y_Z or Chl_Z, giving eq 2

$$[Y_Z^{\bullet}] + [Chl_Z^{\bullet}] = [PSII]_{total} \tag{2}$$

Equations 1 and 2 can be rearranged to

$$\frac{[Y_Z^{\bullet}]}{([PSII]_{total} - [Y_Z^{\bullet}])} = \frac{k_1}{k_2} \tag{3}$$

To examine the Arrhenius behavior of manganese-depleted PSII samples over the pH and temperature ranges examined, the data were plotted to the Arrhenius equation (eq 4),[56] where k is the reaction rate constant, E_a is the activation energy, and A is a preexponential scaling factor

$$\ln k = -\frac{E_a}{RT} + \ln A \tag{4}$$

Given the reasonable assumption that the preexponential factors for the two reactions are equal, the ratio of the corresponding two Arrhenius equations is given by eq 5

$$\ln\left(\frac{[Y_Z^{\bullet}]}{([PSII]_{total} - [Y_Z^{\bullet}])}\right) = \frac{E_{a2} - E_{a1}}{RT} \tag{5}$$

The activation energy and activation enthalpy are related by eq 6

$$E_a = \Delta H^{\ddagger} + RT \tag{6}$$

Therefore

$$E_{a2} - E_{a1} = \Delta H^{\ddagger}_2 - \Delta H^{\ddagger}_1 = \Delta\Delta H^{\ddagger} \tag{7}$$

and

$$\ln\left(\frac{[Y_Z^{\bullet}]}{([PSII]_{total} - [Y_Z^{\bullet}])}\right) * RT = \Delta\Delta H^{\ddagger} \tag{8}$$

According to eqs 4−8,[56] a plot of $\ln([Y_Z^{\bullet}]/([PSII]_{total} - [Y_Z^{\bullet}]))$ as a function of T^{-1} should have a slope of $\Delta\Delta H^{\ddagger}/R$ and, thus, determine the difference in activation enthalpies for $Y_Z^{\bullet}$ versus $Chl_Z^{\bullet}$ formation. If we assume that pH and isotope effects do not alter k_2 or E_{a2}, then we can relate the pH and isotope effects solely to the properties of Y_Z. Indeed, the $Chl_Z^{\bullet}$ formation rate

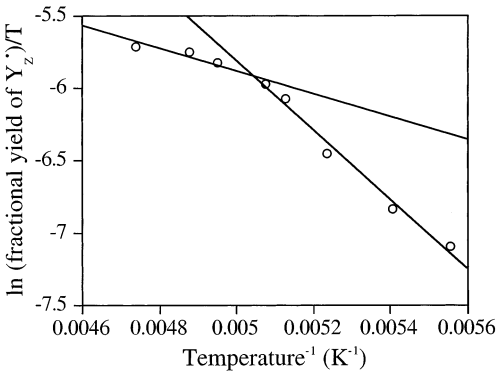

Figure 5. Arrhenius plot of data presented in Figure 2B. The lines represents linear least-squares fits to the first four and last five points, respectively.

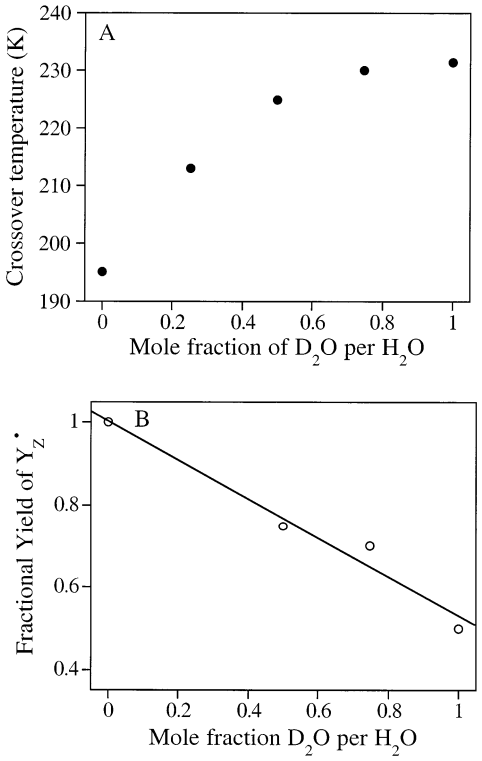

Figure 6. Proton inventory experiment performed at pL 6.0. (A) Crossover temperature, as defined in Figure 2B, versus mole fraction of deuterated water. (B) Fractional yields of $Y_Z^\bullet$ as a function of mole fraction of deuterated water at 230 K. Buffer conditions: 40 mM MES, 10 mM NaCl, 10 mM $CaCl_2$, 300 mM sucrose, 1 mM ferricyanide, and 250 μM DCMU.

was found to be unaffected by pH and isotope conditions over the temperature range examined (Figure 4).[45] Figure 5 shows a representative plot of the data collected at pH 6.5. A quantitative expression for these data is given in eq 8. As is evident from the plot, the data break into two roughly linear phases. Similar behavior is observed at other pH values, except in the extreme low pH regime (not shown). This kind of behavior is not unusual in Arrhenius-type systems and represents accessibility of a second pathway with lower activation energy at higher temperatures. Interestingly, in each case the break occurs at just about 200 K, near the protein-glass transition temperature. This result suggests that as the flexibility of the protein increases and the PCET pathway becomes accessible, the activation enthalpy of $Y_Z^\bullet$ formation is lowered.

Lyonium Isotope Effect. Figure 6A shows that the crossover temperature shifts to higher temperature as the concentration

TABLE 1: $\Delta\Delta H^\ddagger$ Values as a Function of pL[a]

pL	$\Delta\Delta H^\ddagger$ < 200 K in H_2O (kJ mol^{-1})	$\Delta\Delta H^\ddagger$ > 200 K in H_2O (kJ mol^{-1})	$\Delta\Delta H^\ddagger$ > 200 K in D_2O (kJ mol^{-1})
4		15 ± 4	
5		28 ± 1	27 ± 4
5.5	33 ± 3	13 ± 1	
6	22 ± 3	12 ± 1	40 ± 2
6.5	21 ± 1	8 ± 1	
7	11 ± 1		17 ± 1
7.5	8 ± 1		
8	7 ± 2		

[a] pL = − log [lyonium ion], analogous to pH and pD. Not all pH values correspond to both types of $\Delta H^\ddagger$ values, because at low pH (≤ 5) $Y_Z^\bullet$ formation is fully competitive only above 200 K, whereas at high pH (> 7) $Y_Z^\bullet$ formation is fully competitive only below 200 K. The errors represent the uncertainty of the fit to each Arrhenius plot.

of D_2O is increased. To characterize better the retardation of the $Y_Z^\bullet$-formation rate in deuterated water, we quantitated the observed isotope effect (Table 1). Because no rates were measured directly, the k_H/k_D ratio was inferred from the relative yields of $Y_Z^\bullet$ as compared to those of $Chl_Z^\bullet$. These calculations are based on the assumption that the lyonium isotope does not affect $Chl_Z^\bullet$. Indeed, no H/D isotope effect was observed on the rates of radical formation over a temperature range from 150 to 210 K at pH 7 (Figure 4C).[45] To calculate a representative value, the fractional $Y_Z^\bullet$ yield at the crossover temperature in H_2O was divided by the fractional $Y_Z^\bullet$ yield observed at the same absolute temperature in D_2O. The isotope effect thus calculated at the low and high pL extremes (pL ≤ 5 and >7, respectively) is 1.4. At pH 6.0, where activity is greatest,[46] the isotope effect increases to approximately 5.

Several studies performed by Renger and co-workers have focused on the H/D isotope effects of PSII electron transfer, specifically on water oxidation,[57,58] and $P680^+$ reduction.[57,59,60] In laser-induced absorption-change measurements on O_2-evolving PSII, Renger and co-workers observe that at pL 6.5 the rate of $P680^+$ reduction (oxidation of Y_Z) is independent of lyonium isotope, while $Y_Z^\bullet$ reduction by the Mn_4 cluster exhibits an H/D isotope effect of 1.6 to 1.8 in PSII core complexes and of 1.4 in PSII membrane fragments.[57] Rather different results have been obtained from manganese-depleted PSII samples in which a significant H/D isotope effect is observed for the oxidation of Y_Z.[24] The absence of the Mn_4 cluster appears to increase the extent of proton movement required for $Y_Z/Y_Z^\bullet$ redox chemistry. For example, the disruption of favorable hydrogen-bonding networks by depletion of the Mn_4 cluster may necessitate greater proton/protein rearrangements during Y_Z oxidation and $Y_Z^\bullet$ reduction. In measurements on manganese-depleted PSII, the H/D isotope effect has been found to be maximal between pL 6 and 7 ($k_H/k_D = 3-4$) and to be smaller at both higher and lower values of pL.[24] These results on manganese-depleted PSII are in agreement with our findings.

The isotope effect was investigated further in a proton-inventory experiment, where the rate of reaction is correlated to the fraction of deuterons to hydrogens present in the reaction vessel. Figure 6B shows the fractional yield of $Y_Z^\bullet$ as a function of mole fraction of deuterium. These are the first proton-inventory data for PSII. The shape of this plot conveys the number of active protonic sites.[61] A linear relationship indicates that only one proton is required to move in the rate-limiting step, whereas a curved plot points to the movement of two or more protons.[61] We find that the fractional yields follow a straight line. Because the yields are directly proportional to their rate of formation (eq 1), these results provide evidence that only one proton participates in the rate-limiting step.

Discussion

FTIR evidence points toward a hydrogen bond between Y_Z and a histidine side chain.[12] Because $Y_Z^{\bullet}$ is a neutral tyrosyl radical,[10−12] if a proton is associated with reduced Y_Z, then it must be donated to a nearby base as Y_Z is oxidized to $Y_Z^{\bullet}$. Alternatively, Junge and co-workers argue that Y_Z exists as a tyrosinate anion (Y_Z^-) at neutral pH.[13,14] In this case, oxidation of Y_Z would not require movement of a proton. Our finding that one proton is involved in the rate-limiting step for Y_Z oxidation indicates that a proton-coupled electron transfer (PCET) step is necessary for oxidation of Y_Z.

Several studies on PSII mutants have implicated residue D1-His190 as the proton acceptor.[5,7,8,62] Consequently, one major change expected in the environment of Y_Z upon its oxidation is a shift in its hydrogen-bonding interactions. Optical-absorption studies of D1-H190 deficient PSII mutants show that the rates of Y_Z oxidation and $Y_Z^{\bullet}$ reduction are greatly decreased and can be restored by the addition of extrinsic imidazole or other small organic bases. The same was found to be true in manganese-depleted wild-type PSII,[7,9] indicating that in the absence of the Mn_4 cluster, the interaction between Y_Z and D1-His190 is not optimal. If structural perturbations persist in manganese-depleted PSII, proton-coupled electron-transfer steps should be disproportionately affected.

Structural Requirements for PCET. Protein functionality depends on structural flexibility.[26,27,43] The dynamic transition between a glasslike and a less motionally restricted state occurs between 180 and 230 K for most proteins.[25−27] In the present study, we find that the activation enthalpy of $Y_Z^{\bullet}$ radical formation decreases significantly above about 200 K. In intact PSII, electron transfer between Y_Z and $P680^+$ and between the Mn_4 cluster and $Y_Z^{\bullet}$ does not appear to have a significant energetic barrier in the S_1-to-S_2-state transition, as indicated by the finding that this transition can occur at temperatures as low as 140 K.[34] In contrast, in inhibited PSII samples, all of the S-state transitions, including the S_1-to-S_2-state transition, can only occur above illumination temperatures ranging from 200 to 250 K.[63−65] Similarly, in manganese-depleted PSII, $Y_Z^{\bullet}$ is only formed by illumination at temperatures above 230 to 250 K.[35,37] The simplest explanation for this so-called Y_Z paradox is that the removal or perturbation of the Mn_4 cluster significantly alters the hydrogen-bonding environment of the OEC, leading to changes in the redox properties of Y_Z.[66] We propose that two different mechanistic pathways for Y_Z oxidation/$Y_Z^{\bullet}$ reduction are accessible in manganese-containing PSII.[21] The first can occur at low temperature in the S_1-to-S_2-state transition and may involve the low-barrier movement of a proton between Y_Z and a basic residue B, possibly D1-His190, via a well-ordered and strong hydrogen bond. The second requires concerted PCET between the Mn_4 cluster and $Y_Z^{\bullet}$ and can only occur only above 200 K, where thermal motions and nuclear rearrangements become permissible. In manganese-deficient centers, the former mechanism is severely retarded and, therefore, the pathway for $Y_Z^{\bullet}$ formation requires significant proton/protein movement for PCET.

Energetic Advantages of PCET and Thermodynamic Requirements for Hydrogen-Atom Transfer. Our results show that the redox activity of Y_Z is dependent on PCET. Coupling electron transfer to protonic movements may have energetic advantages for the OEC in PSII. In inorganic manganese model complexes, H-atom transfer is directly related to the thermodynamic affinity of the oxidant for $H^{\bullet}$.[67,68] Therefore, coupling the electron-transfer reaction to the movement of a proton can increase the driving force for the reaction.

It is noteworthy that the potential of tyrosines in proteins can be tuned relatively easily by adjustments of their respective microenvironments. The potential of the $Y/Y^{\bullet}$ couple in solution varies from 1.22 at pH 2, to 0.93 at pH 7, and 0.64−0.72 at pH 13 (in V versus NHE).[69,70] $Y_Z^{\bullet}$ is exposed to the bulk solvent in PSII[17,71] and the lumenal side of the membrane can reach pH values of below 5. The low effective local pH near Y_Z may increase the midpoint potential of $Y_Z/Y_Z^{\bullet}$ to significantly above that of $Y_D/Y_D^{\bullet}$ by adjusting charges on the nearby amino acid side chains.[3,72−75]

Indeed, the observed pK_a values for the amino acid residues in question reflect such adjustments. The phenolic hydroxyl group of tyrosine is expected to undergo high-pH acid dissociation with a pK_a of ∼10.[76] Likewise, the putative proton acceptor involved in Y_Z oxidation (denoted B) should dissociate with a specific pK_a, presumably in the acidic pH range. Both of these reactions impact on the efficiency and mechanism of $Y_Z^{\bullet}$ formation. Above the pK_a of Y_Z, where the tyrosinate anion is formed, $Y_Z^{\bullet}$ formation should proceed with great efficiency and without pH or lyonium-isotope dependence, because proton movement is not required to form $Y_Z^{\bullet}$. Unfortunately, this pH range cannot easily be surveyed, because at such high pH other portions of the PSII protein complex begin to fail. Below the pK_a of Y_Z but above the pK_a of its proton-acceptor base B, consecutive PCET can occur by shuttling a proton back and forth between Y_Z and B. Below the pK_a of B, both Y_Z and B are protonated and can no longer form a hydrogen bond or share a proton in PCET. Therefore, the efficiency of $Y_Z^{\bullet}$ formation should diminish below this pH. Indeed, this behavior is observed in the present study, with the efficiency of Y_Z oxidation decreasing dramatically below pH ∼5.5.

Diner, Britt, and co-workers propose the pK_a value of B to be ∼5.[24] Their proposed mechanism of Y_Z oxidation involves proton-coupled electron transfer between pH ∼5 and the pK_a of Y_Z. The titration behavior observed in the present study supports their finding. We observe a donor-side species pK_a of about 5.5, consistent with the range suggested by Diner et al.,[24] and also with the known titration behavior of isolated imidazole and histidine groups.[76] Within a protein, the pK_a of an amino acid side chain can be lowered significantly, making protonation less electrostatically favorable. There is a mechanistic advantage to depressing the pK_a of B, because this residue is proximal to the OEC and likely partially exposed to the lumen. The lumenal pH can decrease to below 5 during maximum PSII activity. The lower the pK_a of the proton-acceptor base to Y_Z, the longer will PCET stay functional as protons accumulate in the lumen and the lumenal pH decreases.

Implications for Future Studies. The method used herein to examine the photooxidation of Y_Z could be expanded to manganese-containing PSII, to study H/D effects on photooxidation of the OEC, similar to the pH dependence studies completed earlier.[28,29] Work on manganese-containing PSII would provide information on the complete donor-side electron-transfer chain and the behavior of the fully functional OEC. As is true for the present work, the yields measured in kinetic competition assays reflect only the rate-determining steps in the photooxidation reaction. Although only a limited portion of the mechanism can thus be examined, our method constitutes a powerful and simple tool to address basic mechanistic questions related to the photochemistry of the donor side of PSII.

Acknowledgment. We thank Dr. John Vrettos for helpful discussions and for critically reading the manuscript. This work was supported by the National Institutes of Health (GM32715).

References and Notes

(1) Debus, R. J. *Biochim. Biophys. Acta* **1992**, *1102*, 269.
(2) Debus, R. J.; Barry, B. A.; Babcock, G. T.; McIntosh, L. *Proc. Natl. Acad. Sci. U.S.A.* **1988**, *85*, 427.
(3) Metz, J. G.; Nixon, P. J.; Rögner, M.; Brudvig, G. W.; Diner, B. A. *Biochemistry* **1989**, *28*, 6960.
(4) Diner, B. A.; Babcock, G. T. In *Oxygenic Photosynthesis: The Light Reactions*; Ort, D., Yocum, C., Eds.; Kluwer Academic Publishers: The Netherlands, 1996; p 213.
(5) Roffey, R. A.; Kramer, D. M.; Govindjee; Sayre, R. T. *Biochim. Biophys. Acta* **1994**, *1185*, 257.
(6) Roffey, R. A.; van Wijk, K. J.; Sayre, R. T.; Styring, S. *J. Biol. Chem.* **1994**, *269*, 5115.
(7) Hays, A.-M.; Vassiliev, I. R.; Golbeck, J. H.; Debus, R. J. *Biochemistry* **1998**, *37*, 11 352.
(8) Mamedov, F.; Sayre, R. T.; Styring, S. *Biochemistry* **1998**, *37*, 14 245.
(9) Hays, A. M. A.; Vassiliev, I. R.; Golbeck, J. H.; Debus, R. J. *Biochemistry* **1999**, *38*, 11 851.
(10) Tommos, C.; Tang, X.-S.; Warncke, K.; Hoganson, C. W.; Styring, S.; McCracken, J.; Diner, B. A.; Babcock, G. T. *J. Am. Chem. Soc.* **1995**, *117*, 10 325.
(11) Noguchi, T.; Inoue, Y.; Tang, X.-S. *Biochemistry* **1997**, *36*, 14 705.
(12) Berthomieu, C.; Hienerwadel, R.; Boussac, A.; Breton, J.; Diner, B. A. *Biochemistry* **1998**, *37*, 10 547.
(13) Ahlbrink, R.; Haumann, M.; Cherepanov, D.; Bögershausen, O.; Mulkidjanian, A.; Junge, W. *Biochemistry* **1998**, *37*, 1131.
(14) Haumann, M.; Mulkidjanian, A.; Junge, W. *Biochemistry* **1999**, *38*, 1258.
(15) Tommos, C.; Hoganson, C. W.; Di Valentin, M.; Lydakis-Simantiris, N.; Dorlet, P.; Westphal, K.; Chu, H. A.; McCracken, J.; Babcock, G. T. *Curr. Op. Struct. Biol.* **1998**, *2*, 244.
(16) Gilchrist, M. L.; Ball, J. A.; Randall, D. W.; Britt, R. D. *Proc. Natl. Acad. Sci. U.S.A.* **1995**, *92*, 9545.
(17) Hoganson, C. W.; Lydakis-Simantiris, N.; Tang, X.-S.; Tommos, C.; Warncke, K.; Babcock, G. T.; Diner, B. A.; McCracken, J.; Styring, S. *Photosynth. Res.* **1995**, *46*, 177.
(18) Hoganson, C. W.; Babcock, G. T. *Science* **1997**, *277*, 1953.
(19) Pecoraro, V. L.; Baldwin, M. J.; Caudle, M. T.; Hsieh, W.-Y.; Law, N. A. *Pure Appl. Chem.* **1998**, *70*, 925.
(20) Limburg, J.; Szalai, V. A.; Brudvig, G. W. *J. Chem. Soc., Dalton Trans.* **1999**, 1353.
(21) Vrettos, J. S.; Limburg, J.; Brudvig, G. W. *Biochim. Biophys. Acta* **2001**, *1503*, 229.
(22) Babcock, G. T.; Sauer, K. *Biochim. Biophys. Acta* **1975**, *396*, 48.
(23) Yerkes, C. T.; Babcock, G. T. *Biochim. Biophys. Acta* **1980**, *590*, 360.
(24) Diner, B. A.; Force, D. A.; Randall, D. W.; Britt, R. D. *Biochemistry* **1998**, *37*, 17 931.
(25) Doster, W.; Cusack, S.; Petry, W. *Nature* **1989**, *337*, 754.
(26) Rasmussen, B. F.; Stock, A. M.; Ringe, D.; Petsko, G. A. *Nature* **1992**, *357*, 423.
(27) Ferrand, M.; Dianoux, A. J.; Petry, W.; Zaccai, G. *Proc. Natl. Acad. Sci. U.S.A.* **1993**, *90*, 9668.
(28) de Paula, J. C.; Innes, J. B.; Brudvig, G. W. *Biochemistry* **1985**, *24*, 8114.
(29) Thompson, L. K.; Brudvig, G. W. *Biochemistry* **1988**, *27*, 6653.
(30) Miller, A.-F.; Brudvig, G. W. *Biochim. Biophys. Acta* **1991**, *1056*, 1.
(31) Hanley, J.; Deligiannakis, Y.; Pascal, A.; Faller, P.; Rutherford, A. W. *Biochemistry* **1999**, *38*, 8189.
(32) Tracewell, C. A.; Vrettos, J. S.; Bautista, J. A.; Frank, H. A.; Brudvig, G. W. *Arch. Biochem. Biophys.* **2001**, *385*, 61.
(33) Tracewell, C. A.; Cua, A.; Stewart, D. H.; Bocian, D. F.; Brudvig, G. W. *Biochemistry* **2001**, *40*, 193.
(34) Casey, J. L.; Sauer, K. *Biochim. Biophys. Acta* **1984**, *767*, 21.
(35) Kodera, Y.; Takura, K.; Mino, H.; Kawamori, A. In *Research in Photosynthesis*; Murata, N., Ed.; Kluwer Academic Publishers: The Netherlands, 1992; p 57.
(36) Szalai, V. A.; Brudvig, G. W. *Biochemistry* **1996**, *35*, 1946.
(37) Shigemori, K.; Mino, H.; Kawamori, A. *Plant Cell Physiol.* **1997**, *38*, 1007.
(38) Mino, H.; Astashkin, A. V.; Kawamori, A. *Spectrochim. Acta A* **1997**, *53*, 1465.
(39) Mino, H.; Kawamori, A.; Ono, T. *Biochim. Biophys. Acta* **2000**, *1457*, 157.
(40) Brudvig, G. W.; Casey, J. L.; Sauer, K. *Biochim. Biophys. Acta* **1983**, *723*, 366.
(41) Koike, H.; Hanssum, B.; Inoue, Y.; Renger, G. *Biochim. Biophys. Acta* **1987**, *893*, 524.
(42) Horgan, D. J.; Kurth, L. B.; Kuypers, R. *J. Food Sci.* **1991**, *56*, 1203.
(43) Réat, V.; Patzelt, H.; Ferrand, M.; Pfister, C.; Oesterhelt, D.; Zaccai, G. *Proc. Natl. Acad. Sci. U.S.A.* **1998**, *95*, 4970.
(44) Jermyn, M. A. *Aust. J. Chem.* **1967**, *20*, 183.
(45) Kühne, H. 2000 Ph.D. thesis, Yale University, New Haven.
(46) Berthold, D. A.; Babcock, G. T.; Yocum, C. F. *FEBS Lett.* **1981**, *134*, 231.
(47) Beck, W. F.; de Paula, J. C.; Brudvig, G. W. *Biochemistry* **1985**, *24*, 3035.
(48) Tamura, N.; Cheniae, G. *Biochim. Biophys. Acta* **1987**, *890*, 179.
(49) Arnon, D. I. *Plant Physiol.* **1949**, *24*, 1.
(50) Pentz, L.; Thornton, E. R. *J. Am. Chem. Soc.* **1967**, *89*, 6931.
(51) Razeghifard, M. R.; Klughammer, C.; Pace, R. J. *Biochemistry* **1997**, *36*, 86.
(52) Faller, P.; Debus, R. J.; Brettel, K.; Sugiura, M.; Rutherford, A. W.; Boussac, A. *Proc. Natl. Acad. Sci. U.S.A.* **2001**, *98*, 14 368.
(53) Stewart, D. H.; Cua, A.; Chisholm, D. A.; Diner, B. A.; Bocian, D. F.; Brudvig, G. W. *Biochemistry* **1998**, *37*, 10 040.
(54) Vrettos, J.; Stewart, D. H.; de Paula, J. C.; Brudvig, G. W. *J. Phys. Chem. B* **1999**, *103*, 6403.
(55) Boska, M.; Sauer, K.; Buttner, W.; Babcock, G. T. *Biochim. Biophys. Acta* **1983**, *722*, 327.
(56) Segel, I. H. *Enzyme Kinetics—Behavior and Analysis of Rapid Equilibrium and Steady-State Enzyme Systems*; Wiley-Interscience: New York, 1993.
(57) Karge, M.; Irrgang, K.-D.; Sellin, S.; Feinäugle, R.; Liu, B.; Eckert, H.-J.; Eichler, H. J.; Renger, G. *FEBS Lett.* **1996**, *378*, 140.
(58) Karge, M.; Irrgang, K.-D.; Renger, G. *Biochemistry* **1997**, *36*, 8904.
(59) Haumann, M.; Bögershausen, O.; Cherepanov, D.; Ahlbrink, R.; Junge, W. *Photosynth. Res.* **1997**, *51*, 193.
(60) Christen, G.; Seeliger, A.; Renger, G. *Biochemistry* **1999**, *38*, 6082.
(61) Venkatasubban, K. S.; Schowen, R. L. *CRC Crit. Rev. Biochem.* **1984**, *17*, 1.
(62) Nixon, P. J.; Diner, B. A. *Biochem. Soc. Trans.* **1994**, *22*, 338.
(63) Beck, W. F.; de Paula, J. C.; Brudvig, G. W. *J. Am. Chem. Soc.* **1986**, *108*, 4018.
(64) Beck, W. F.; Brudvig, G. W. *Biochemistry* **1986**, *25*, 6479.
(65) Ono, T.-A.; Zimmermann, J.-L.; Inoue, Y.; Rutherford, A. W. *Biochim. Biophys. Acta* **1986**, *851*, 193.
(66) Babcock, G. T.; Espe, M.; Hoganson, C.; Lydakis-Simantiris, N.; McCracken, J.; Shi, W.; Styring, S.; Tommos, C.; Warncke, K. *Acta Chem. Scand.* **1997**, *51*, 533.
(67) Gardner, K. A.; Mayer, J. M. *Science* **1995**, *269*, 1849.
(68) Wang, K.; Mayer, J. M. *J. Am. Chem. Soc.* **1997**, *119*, 1470.
(69) Jovanovic, S. V.; Harriman, A.; Simic, M. G. *J. Phys. Chem.* **1986**, *90*, 1935.
(70) Harriman, A. *J. Phys. Chem.* **1987**, *91*, 6102.
(71) Tang, X.-S.; Zheng, M.; Chisholm, D. A.; Dismukes, G. C.; Diner, B. A. *Biochemistry* **1996**, *35*, 1475.
(72) Boussac, A.; Etienne, A. L. *Biochim. Biophys. Acta* **1984**, *766*, 576.
(73) Babcock, G. T.; Barry, B. A.; Debus, R. J.; Hoganson, C. W.; Atamian, M.; McIntosh, L.; Sithole, I.; Yocum, C. F. *Biochemistry* **1989**, *28*, 9557.
(74) Vass, I.; Styring, S. *Biochemistry* **1991**, *30*, 830.
(75) Baldwin, M. J.; Pecoraro, V. L. *J. Am. Chem. Soc.* **1996**, *118*, 11 325.
(76) Creighton, T. E. *Proteins—Structures and Molecular Properties*; W. H. Freeman and Company: New York, 1993.